

Comparative Safety Assessment of Automated Driving Strategies at Highway Merges in Mixed Traffic

Mullakkal-Babu, F. A.; Wang, M.; Arem, B. van; Happee, R.

DOI

[10.1109/TITS.2020.3038866](https://doi.org/10.1109/TITS.2020.3038866)

Publication date

2020

Document Version

Final published version

Published in

IEEE Transactions on Intelligent Transportation Systems

Citation (APA)

Mullakkal-Babu, F. A., Wang, M., Arem, B. V., & Happee, R. (2020). Comparative Safety Assessment of Automated Driving Strategies at Highway Merges in Mixed Traffic. *IEEE Transactions on Intelligent Transportation Systems*, 23(4), 3626-3639. <https://doi.org/10.1109/TITS.2020.3038866>

Important note

To cite this publication, please use the final published version (if applicable).
Please check the document version above.

Copyright

Other than for strictly personal use, it is not permitted to download, forward or distribute the text or part of it, without the consent of the author(s) and/or copyright holder(s), unless the work is under an open content license such as Creative Commons.

Takedown policy

Please contact us and provide details if you believe this document breaches copyrights.
We will remove access to the work immediately and investigate your claim.

Green Open Access added to TU Delft Institutional Repository

'You share, we take care!' - Taverne project

<https://www.openaccess.nl/en/you-share-we-take-care>

Otherwise as indicated in the copyright section: the publisher is the copyright holder of this work and the author uses the Dutch legislation to make this work public.

Comparative Safety Assessment of Automated Driving Strategies at Highway Merges in Mixed Traffic

Freddy Antony Mullakkal-Babu^{ID}, Meng Wang^{ID}, *Member, IEEE*,
Bart van Arem^{ID}, *Senior Member, IEEE*, and Riender Happee^{ID}

Abstract—We present a simulation-based approach to assess the safety impacts of vehicles equipped with Automated Driving Systems (ADS) in mixed traffic with Human-driven Vehicles (HV). Specifically, we compare two generic longitudinal strategies of ADS to handle a cut-in: Reactive ADS acting only when the cut-in vehicle crosses the target lane boundary, and Predictive ADS acting at the onset of the cut-in manoeuvre. We identify their distinctive effects on the traffic safety under cut-in maneuvers of adjacent human-driven vehicles at highway merges. We employ a microscopic traffic flow simulator that describes the lane changing process with high detail, accounting for the vehicle interaction and consequent trajectory updates. These high-resolution trajectories are post-processed to estimate a set of relevant surrogate measures of safety. By analyzing these measures, we find that the predictive ADS significantly outperforms the reactive ADS in aspects such as temporal proximity to crash, expected crash severity and the driving risk (combining the two aspects), and the number of aborted lane changes by HV. The negative safety impact of reactive ADS becomes prominent at penetration rate $> 10\%$. The major difference between the two ADS approaches appears in the dynamics of risk during the lane changing. When a vehicle cuts in ahead of Reactive ADS, the risk peaks approximately halfway through the maneuver; whereas with Predictive ADS the risk remains marginal throughout. This work demonstrates the potential of simulation-based safety assessment to differentiate the safety impacts of automation functionalities at an early stage of product development.

Index Terms—Traffic safety, surrogate measure of safety, microscopic simulation, automated driving, tactical decisions.

I. INTRODUCTION

AUTOMATED Driving Systems (ADSs) have been a prominent subject of research and development during

Manuscript received November 18, 2019; revised July 6, 2020 and September 25, 2020; accepted November 9, 2020. This work was supported by the Nederlandse Organisatie voor Wetenschappelijk Onderzoek (NWO) Domain Toegestane en Technische Wetenschappen (TTW) through the Project from Individual Automated Vehicles to Cooperative Traffic Management (IAVTRM). The Associate Editor for this article was L. Li. (*Corresponding author: Meng Wang.*)

Freddy Antony Mullakkal-Babu, Meng Wang, and Bart van Arem are with the Department of Transport and Planning, Faculty of Civil Engineering and Geosciences, Delft University of Technology, 2628 Delft, The Netherlands (e-mail: f.a.mullakkalbabu@tudelft.nl; m.wang@tudelft.nl; b.vanarem@tudelft.nl).

Riender Happee is with the Department of Cognitive Robotics, Faculty of Mechanical, Maritime and Material Engineering, Delft University of Technology, 2628 Delft, The Netherlands (e-mail: r.happee@tudelft.nl).

Digital Object Identifier 10.1109/TITS.2020.3038866

the past three decades. An ADS, when engaged, drives the vehicle without human intervention or monitoring [1]. Market trends indicate that ADS features will be technologically feasible in the near future [2] and the road-traffic will be *mixed* with ADS equipped and human-driven vehicles for a few decades [3]. According to the standard taxonomy, engaged ADS should perform all the driving tasks necessary to operate the vehicle, in real-time on a sustained basis [1]. The driving tasks at tactical-level include event detection, maneuver decision-making and at operational level include acceleration and steering control. The impacts of ADS-equipped vehicles on traffic safety cannot be generalized as ADSs differ in their tactical-level and operational-level functionalities to tackle on-road conflicts. In this context, identifying the relationship between the ADS strategies and traffic safety has gained increased research attention.

A. Safety Assessment Approaches for ADS-Equipped Vehicles

Safety of vehicle applications has been assessed either at the vehicle-level, based on their potential to reduce the number of crashes or at the traffic-level based on their potential impacts on collective traffic safety.

An exhaustive review of vehicle-level studies was provided in [4] which focused on the crash-reduction potential of vehicle applications. Such studies estimate the effectiveness of an application based on the crash involvement rate of the equipped vehicle. The crash recordings may be derived directly from empirical sources such as accident records [5] or from in-lab experiments by reconstructing a set of pre-crash scenarios that are identified from empirical sources [6]. Empirical crash records provide valuable insights into the safety performance of a given vehicle application, but crash data of ADS-equipped vehicles are rare and often confidential. In-lab crash reconstruction experiments, mostly comprise a standard set of traffic situations where the behavior of neighboring vehicles is predefined. Such a setting is not representative of on-road situations, as it does not account for the interactions with the adjacent vehicles [7], and the consequent variations in the trajectory of the vehicles. These interactions are fundamental to the dynamics of multi-lane traffic flow, and the performance of automated driving applications in laboratory experiments may not reveal their actual impact on traffic.

Traffic simulators are potential tools to evaluate the safety impacts of a vehicle application at the traffic-level. The simulated trajectories (of equipped and non-equipped vehicles) are post-processed to derive metrics known as Surrogate Measure of Safety (SMoS). These metrics are analyzed to find safety impacts. The majority of traffic safety studies focussed on the connected vehicle applications and their results consistently suggest that connectivity, if realized will improve the traffic safety [4], [8]–[10]. However, connectivity technology is not yet mature to be widely utilized by ADSs and their prospects are determined by the number of vehicles that can communicate [11], [12]. Hence, on-board sensors remain the primary source of information for ADSs. Notably, the safety impacts of non-connected ADSs have been less studied compared to their connected counterparts [13], [14]. Most of the simulation-based studies, irrespective of the assumption on connectivity, express safety as the reduction in the likelihood of rear-end crashes, based on metrics such as Time-To-Collision [8], [10], [14]–[16] with very few exceptions [13], [17] where lateral conflicts are evaluated. Recently, based on the crash record of vehicles with level 3/4 automation, it is identified that crashes caused by equipped vehicles are likely to be more severe than those of non-equipped vehicles, and that equipped vehicle crashes are more severe on highways [18]. Besides, in comparison to urban roads, an equipped vehicle on a highway is more likely to be involved in angular and sideswipe crashes (mostly related to lane-changes). These findings highlight the need to examine highway lateral conflicts involving ADS equipped vehicles in more detail.

Lateral conflicts on a highway form a challenging subject for safety assessment, particularly those involving ADS-equipped vehicles. This is due to simulator-related and assessment-related challenges. In most of the traffic simulators, the lane change execution is represented as an open-loop process, disregarding the vehicle's interaction with adjacent vehicles during lane-changing execution. In reality, the lane-changing vehicle may dynamically update its lane-changing trajectory and may even abort the maneuver in unsafe situations. However, such instances of lane change abortion cannot be modeled in typical traffic simulators. Second, simulators often do not provide an accessible and flexible framework to model an ADS architecture. Several previous works modeled ADS by adjusting the default behavioral model of the simulators such as VISSIM, CORSIM and SUMO [9], [17], [19]. However, these approaches may fail to capture the differences between ADS-equipped and conventional vehicles with respect to sensing, decision-making and vehicle control. Common trajectory simulations are not sufficiently realistic for safety analysis. For instance, lane-changing is typically simulated as an event during which the vehicle jumps/drifts between two lanes, being unresponsive to the actions of adjacent vehicles. Such a synthetic trajectory does not provide realistic variables such as lateral position and lateral velocity necessary to estimate relevant SMoS. Realistic simulation of lateral kinematics and appropriate selection of SMoS are identified as necessary preconditions to compare the level of safety of two-dimensional trajectories [20].

B. Automated Driving Strategies to Handle Cut-In

One of the critical events that an ADS should handle while operating on a multi-lane highway, is a cut-in, i.e. when an adjacent vehicle pulls in ahead by merging into its lane [21]. When a vehicle is cut in by an adjacent one, its inter-vehicle spacing decreases around 50%. If a vehicle fails to brake effectively when being cut in, it could crash with the merging (cut-in) vehicle. This can be a major concern on highway merging sections, where cut-ins are more frequent. It was reported that approximately 10% of light vehicle crashes involve a lane-changing vehicle [22]. To effectively respond to a cut-in, the ADS should be informed in real-time of the cut-in maneuver: intention, start and end of the maneuver.

To handle a cut-in event, the ADS should perform two tactical tasks: detect (predict) the vehicle that cuts in (the intention of an adjacent vehicle to cut-in); decide on the appropriate response. ADS' response to a cut-in is typically operationalized by its submodule: Adaptive Cruise Control (ACC). ACC systems command the acceleration to regulate the vehicle's velocity to follow the preceding vehicle with a safe spacing and desired speed. Table I describes the two generic approaches adopted by an ADS to handle a cut-in: reactive control and predictive control. In reactive control, the equipped vehicle identifies a cut-in when it detects another vehicle in its lane at a closer spacing than the preceding vehicle it was originally following. Thereafter, the component ACC system generates commands to follow the cut-in vehicle. Several ADS designs adopt the reactive approach [23], [24]. The disadvantage of this approach is that the sudden drop in inter-vehicle spacing often results in hard braking, which is uncomfortable for the driver [23], [24]. Empirical evidence shows that the behavior of the vehicle with ACC-engaged during cut-in, often scares the driver, forcing him/her to take back the control [25].

In the predictive control, the system predicts the cut-in intentions of the adjacent vehicles and identifies the adjacent vehicle which is most likely to cut-in. Several methods to predict the cut-in have been proposed as listed in Table I: turn signal-based [26]; learning-based approaches [11], [27], [28]; Bayesian statistics-based approaches [29], [30]. Upon cut-in prediction, the most appropriate maneuver is calculated taking into account the predicted future motion of the cut-in candidate. Table I summarizes the prominent methods for maneuver decision-making, such as following the virtual leader [26], rule-based [19], [31], utility-based [11], [27], [29], [32] and game theory-based [33], [34]. The underlying motion prediction logic can be kinematic extrapolation based on constant velocity [32]; constant acceleration [11], [27], [29]; or model-based prediction accounting for vehicle interactions [33]. Predictive control allows an early response to cut-in, providing a temporal margin to smoothly regulate the vehicle's velocity to approach the cut-in vehicle. However, the implementation of the predictive approach entails additional computational expense and sensing requirements. Therefore, understanding the safety implications of these systems will facilitate an informed choice between the two approaches.

TABLE I
REVIEW SUMMARY OF CUT-IN HANDLING FUNCTIONALITIES IN ADS

Functionality	Reactive handling	Predictive handling
Cut-in detection/prediction (tactical-level)	radar-based detection [15]	turn signal-based intent prediction [26] learning-based intend prediction [11], [27], [28] bayesian statistics-based intent prediction [29], [30]
Motion prediction for adjacent vehicles (tactical-level)	N.A.	constant velocity [32] constant acceleration [11], [27], [29] interaction-aware prediction [33]
maneuver decision (tactical-level)	follow the cut-in vehicle [15], [23], [24]	follow the virtual leader [26] rule-based yielding [31], [19] expected utility-based maneuver planning [11], [27], [29], [32] game theory-based maneuver planning [33], [34]
Acceleration control (operational-level)	feedback gain based control [23], [24]	feedback gain based control [26] optimal control [27], [32]

The ADS' cut-in handling functionalities have been typically tested based on crash-reduction potential by simulation and/or by test vehicles. The results show that they could decrease the number of events with hard-braking and reduce the average Time-To-Collision [14]. Few attempts have been found to estimate their impact on traffic safety. At the traffic level, it was found that ACC systems with a conservative target time-headway (≥ 1.2 s), may result in more spacing between vehicles and thereby invite more cut-ins [35]. Bhram *et al.* [14] simulated ADS with a reactive approach. They found that such systems create more risky situations, but the risk is dispensed faster than human-driven vehicles. Moreover, they suggested that few crashes in the simulation could have been avoided if these systems had prediction capability. But none of these studies examine the impacts of cut-in handling functionalities on the safety of lateral conflicts and the consequences of the vehicle interaction during the cut-in maneuver.

C. Objective, Contribution and Structure

The objective of this work is to present a simulation-based safety assessment methodology to assess the impacts of ADS's longitudinal functionality on the safety and characteristics of lateral maneuvers by adjacent human-driven vehicles on the highway. We apply this methodology to compare the reactive and predictive cut-in handling by ADS to facilitate an informed choice between them. Towards this, we employ a microscopic traffic simulator that provides continuous two-dimensional vehicle trajectories capturing dynamic lane-change re-planning. The simulated vehicle trajectories are post-processed to estimate surrogate metrics of safety (SMoS) characterising the conflicts with adjacent vehicles, expected crash severity and dynamics of the driving risk. In addition, we identify the change in lane change characteristics in terms of the frequency of non-successful lane changes, spatial distribution and average velocity. Based on simulations of several traffic scenarios, we delineate and compare the distinct trends in the safety metrics and lane changing characteristics under the increasing share of two types of ADSs.

The contribution of the work is threefold. First, it uses a recently developed traffic simulation framework that

models the lane change decision and execution as a feedback process [36]. It captures failures of lane change maneuvers (abortions) and generates realistic 2D maneuvers taking into account vehicle dynamics. The prediction of lane change abortions is used as a new indicator to quantify turbulence at highway merges. Second, we employ our new Probabilistic Driving Risk Field (PRDF), which is predictive in nature and captures the motion uncertainties of surrounding vehicles. PRDF was shown to be more generic than existing surrogate measures of safety in simple scenarios [37], and the current paper demonstrates that PRDF can be effectively used to analyze conflicts in large scale traffic simulations. Last, the simulation results of the two generic design strategies of ADS, being reactive and predictive, give new insights in the potential benefits and risks of such systems at the collective traffic level. This sheds lights for public authorities and industry to design and manage the emerging technologies to maximize their societal benefits and minimize associated risks.

The simulation framework, notations and mathematical formulation of the distinct cut-in handling approaches employed by ADS-equipped vehicles and Human-driven Vehicle (HV) are described in Section II. In section III, a set of metrics for safety analysis are selected. Section IV presents the results of the case study, followed by Sensitivity analysis in Section V. Finally, Section VI presents conclusions and outlines future research.

II. MODEL FORMULATION

This section presents three distinct models for cut-in handling and describes the model for manual lane-changing. To meet the research objective, two requirements were imposed on the microscopic traffic simulator: 1) it should describe both HV and ADS-equipped vehicles and their specific tactical-level and operational-level functions; 2) it should describe the two-dimensional lane-changing trajectory accounting for dynamic maneuver re-planning during a lane change.

The dynamic state of a vehicle i (point mass) is described by its position vector \mathbf{p}^i defined as $\mathbf{p}^i = [x^i, y^i]^T$, where x^i denotes longitudinal position, and y^i denotes lateral position of the vehicle's center of mass; and velocity vector \mathbf{v}^i defined as

$\mathbf{v}^i = [v_x^i, v_y^i]^T$, where v_x^i denotes longitudinal velocity, and v_y^i denotes lateral velocity. The control unit of vehicle i dynamically manipulates its state implementing an acceleration as the input vector \mathbf{a}^i defined as $\mathbf{a}^i = [a_x^i, a_y^i]^T$, where a_x^i denotes longitudinal acceleration and a_y^i denotes lateral acceleration. The dynamic relation of this system can be expressed in the state space form as

$$\frac{d}{dt} \begin{pmatrix} \mathbf{p} \\ \mathbf{v} \end{pmatrix} = \begin{bmatrix} 0 & 1 \\ 0 & 0 \end{bmatrix} \cdot \begin{pmatrix} \mathbf{p} \\ \mathbf{v} \end{pmatrix} + \begin{pmatrix} 0 \\ 1 \end{pmatrix} \cdot \mathbf{a} \quad (1)$$

The vehicle geometry is assumed to be a rectangle of length l and width w . The physical limitations of the vehicle motion are implemented as a set of feasibility constraints in the model. The velocity is constrained by $-0.17v_x \leq v_y \leq 0.17v_x$, to depict the nonholonomic behavior of motor vehicles [38], and additionally by $v_x \geq 0$ assuming the vehicles move strictly in the forward direction. The mechanical limitations of the vehicle are modeled by bounding the acceleration $a_{min} \leq a_x \leq a_{max}$, where a_{max} denotes the maximum and a_{min} the minimum feasible acceleration. In a cut-in event, the vehicle that is being cut in, performs two tactical-level tasks: cut-in event detection denoted by ζ , yield decision denoted by γ and employs a_x to operationalize the decision. The vehicle, that cuts in, performs the tactical-level lane change decision denoted by ξ and employs \mathbf{a} to operationalize the decision. The following are the key assumptions in the study,

- [1] The ADS-equipped vehicle operates only in the longitudinal direction and does not change lane. Modeling the sustained automation of the longitudinal driving task is sufficient to meet the objective of this study.
- [2] The human-driven vehicle can change lane and can estimate the acceleration of adjacent equipped and non-equipped vehicles and thereby calculate the utility of a prospective lane change.

A. Acceleration Models to Follow the Predecessor

The longitudinal acceleration behavior of HV and ADS-equipped vehicles are differentiated by modelling them with distinct control laws.

1) *Acceleration Model of ADS-Equipped Vehicle*: The longitudinal acceleration implemented by an ADS-equipped vehicle to follow a leader is formulated by the ACC law in a previous work [24]. This control law integrates both ACC and collision avoidance control in a single non-linear formulation, and yield smooth acceleration behavior in a cut-in or when the leader brakes hard. The longitudinal acceleration input by the ACC law a_{ACC}^i is formulated as

$$a_{ACC}^i(\alpha) = \begin{cases} K_1 s_e - K_2 \Delta v_x^i(\alpha) R(s^i(\alpha)), & \text{if } s^i(\alpha) > r_f \\ K_3 (v^d - v_x^i), & \text{if } s^i(\alpha) \leq r_f \end{cases} \quad (2)$$

where α is the vehicle (ADS-equipped or Human driven) preceding i , v^d is the desired velocity of i , $s^i = x^\alpha - x^i - l$ is the space gap available to i with l denoting the length of the α , $\Delta v_x = v_x^i - v_x^\alpha$ is the velocity difference of i with respect to the vehicle α , r_f is the detection range of i 's forward sensor, K_1 K_2 and K_3 are the control gains. The s_e is the spacing

error defined as

$$s_e = \min \left\{ s^i - s_0 - v_x^i \cdot t_d, (v_0 - v_x^i) \cdot t_d \right\} \quad (3)$$

where t_d is the desired time headway, s_0 is the minimum space gap. $R(s^i)$ is a sigmoidal function in s^i that enables collision avoidance, by evoking a strong braking response when approaching the leader at short space gap and a milder response when the leader is further away. R is defined as

$$R = \frac{-1}{1 + Qe^{-\left(\frac{s^i}{J}\right)}} + 1 \quad (4)$$

where Q and J are parameters determining the aggressiveness of the response.

2) *Model for Manual Car-Following*: The longitudinal acceleration implemented by a human driver following a predecessor is formulated by the Intelligent Driver Model [39]. IDM is a behavioral model in which the acceleration is a continuous function of the space gap and velocity difference of i w.r.t α . This model has been widely used to describe manual acceleration behavior and to replicate emergent traffic phenomena such as capacity drop and congestion waves. The longitudinal acceleration input by IDM a_{IDM}^i is formulated as

$$a_{IDM}^i(\alpha) = \bar{a} \left[1 - \left(\frac{v_x^i}{v_d} \right)^4 - \left(\frac{s^*(v_x^i, \Delta v_x^i(\alpha))}{s^i(\alpha)} \right)^2 \right] \quad (5)$$

where \bar{a} denotes the maximum acceleration. s^* denotes the desired minimum space gap as follows

$$s^* = s_0 + v_x^i t_d + \frac{\Delta v_x^i(\alpha)}{2\sqrt{ab}} \quad (6)$$

where b is the comfortable braking.

B. Acceleration Models With Cut-In Handling

In the previous section, we presented the models of a_x^i when the sole objective of i is to follow one leader α . In a cut-in, i confronts two vehicles: the preceding vehicle $i+1$ and the merging vehicle c . It should gradually transition from following-the-leader to following-the-merging-vehicle, meanwhile avoiding a crash.

First, we present the notations used to describe cut-in handling and label the relevant vehicles. Let σ^i be a discrete variable denoting the current lane number as $\sigma^i \in \{1, 2, \dots, L\}$, with 1 denoting the leftmost lane and L denoting the total number of lanes. Let ξ^i be a discrete variable denoting the lane change direction of vehicle i with $\xi^i \in \{+1, 0, -1\} := \{\text{move to the right lane, remain in the current lane, move to the left lane}\}$. Let ζ^i be a binary variable with $\zeta^i \in \{1, 0\}$ such that $\zeta^i = 1 := i$ is being cut in if there exists a vehicle c defined as

$$\zeta^i = \begin{cases} 1, & \text{if } \exists c, \text{ s.t. } x^{i+1} \geq x^c \geq x^i \text{ and } \sigma^i - \sigma^c = \xi^c \\ 0, & \text{otherwise} \end{cases} \quad (7)$$

where c is the vehicle that cuts in i , and $i+1$ is the vehicle preceding i in its lane.

In the remainder of this section, we formulate three models for cut-in handling: reactive and predictive (for ADS-equipped

vehicle) and manual (for HV). These models differentiate between the vehicles at tactical-level and control-level: 1) the forward and backward distance on the adjacent lane that can be sensed by i denoted by r_a^i symmetric in both directions (tactical-level); 2) the logic of an additional leader from the adjacent vehicles that are likely to cut in (tactical-level); 3) the logic to decide whether or not to yield to the cut-in vehicle (tactical-level) 4) the acceleration control employed to handle a cut-in (control-level). The manual cut-in handling differs from ADS cut-in handling at both levels. Among ADS-equipped vehicle models, the reactive and predictive differ in all except the first feature. They have the same sensing range of $r_a = 200$ m. The cut-in handling models are generic extensions of the respective acceleration models formulated in Section II-A, with additional variables to switch to a new leader or include an additional leader in the control law or even switch between two control laws to handle a cut-in. In the remainder of the paper, we refer to ADS-equipped vehicles that employ reactive control simply as Reactive ADS and those which employ predictive control as Predictive ADS.

1) *Model With Reactive Cut-In Handling*: A Reactive ADS detects a cut-in only when the cut-in vehicle crosses the target lane boundary. The binary variable ζ_R^i with $\zeta_R^i \in \{1, 0\}$ denotes whether the cut-in is detected, such that $\zeta_R^i = 1 := i$ detects the cut in, based on the conditions formulated as

$$\zeta_R^i = \begin{cases} 1, & \text{if } \zeta^i = 1 \text{ and} \\ & x^c \leq x^i + r_a \text{ and } |\Delta y(i, c)| \leq W \cdot 0.5 \\ 0, & \text{otherwise} \end{cases} \quad (8)$$

This formulation includes two conditions: 1) The cut-in should occur with the sensing range of i , represented as $x^c \leq x^i + r_a$; 2) the center of mass of c should cross the boundary of σ^i represented as $|\Delta y(i, c)| \leq W \cdot 0.5$, where W denotes the lane width. The detection condition ζ_R^i is then added to the control law to model the generic acceleration a_{RH} with reactive cut-in handling as

$$a_{RH}^i = \min \{a_{ACC}(i+1), \zeta_R^i \cdot a_{ACC}(c)\} \quad (9)$$

where $i+1$ is the vehicle preceding i in its current lane and c is the cut-in vehicle.

2) *Model With Predictive Cut-In Handling*: Compared to a reactive system, the predictive system possesses enhanced detection capabilities. Let ζ_P^i be a binary variable with $\zeta_P^i \in \{1, 0\}$, denotes whether the cut-in is detected, such that $\zeta_P^i = 1 := i$ detects the cut in, based on the conditions formulated as

$$\zeta_P^i = \begin{cases} 1, & \text{if } \zeta^i = 1 \text{ and } x^c \leq x^i + r_a \\ 0, & \text{otherwise} \end{cases} \quad (10)$$

This formulation includes only a single condition that cut-in should occur within i 's sensing range. The distinction in the moments (during cut-in) when the event is detected by reactive and predictive ADS-equipped vehicle is illustrated in Figure 1. At the moment depicted in Figure 1(a), the cut-in event is not detected by reactive ADS-equipped vehicle, whereas at the moment in Figure 1(b) the event is detected.

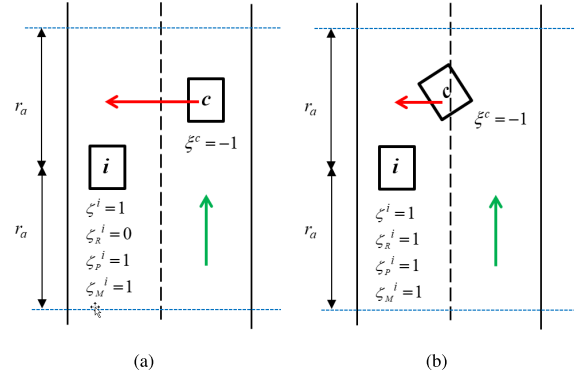


Fig. 1. Example illustration of cut-in events (a) cut-in detected by Predictive ADS and HV (b) cut-in detected by all vehicle types.

Besides cut-in detection, a predictive system possesses additional functionalities. While approaching a highway merging section on the rightmost lane, the predictive ADS-equipped vehicle selects an adjacent vehicle that is likely to merge and switches its acceleration control to yield for the selected vehicle within its predicted time of entry in the acceleration lane.

Let \mathbb{O} be the set of vehicles $o \in \mathbb{O}$ present on the on-ramp with $\mathbb{O} : o \in \mathbb{O} | \sigma^o = \sigma^{ramp}$, with σ^{ramp} denoting the lane number of on-ramp. A predictive ADS-equipped vehicle considers a set of adjacent vehicles \mathbb{A}_P on the on-ramp $\mathbb{A}_P \subset \mathbb{O}$, within its sensor range, i.e. $\mathbb{A}_P \ni a | x^i + r_a^S \geq x^a \leq x^i - r_a^S$. Thereafter, it selects a vehicle g from \mathbb{A}_P based on the selection rule: $g \in \mathbb{A}_P | x^{i+1} \geq x^g$ and $s(i, g) = \max \{s(i, a) | a \in \mathbb{A}_P\}$. This rule prescribes that g should be i 's far most adjacent vehicle which is behind $i+1$. The far-most vehicle is selected as it would be the first vehicle to reach the acceleration zone and thereby the first vehicle that can cut-in among all the adjacent vehicles. Yielding to nearer adjacent vehicles would cost larger velocity loss for i . Figure 2(a) illustrates the selection of g in an example traffic situation.

The future state of g depicted as $\{x^{g*}, v_x^{g*}\}$ are predicted at discrete time steps as $\mathbf{x}^{g*} = (x_1^{g*}, x_2^{g*}, \dots, x_P^{g*})^T$ and $\mathbf{v}_x^{g*} = (v_{x,1}^{g*}, v_{x,2}^{g*}, \dots, v_{x,P}^{g*})^T$ where P is the finite prediction time horizon. The following sets of equation are used to predict the future states of g over the discrete time instances k .

$$\begin{aligned} x^{g*}(k+1) &= x^{g*}(k) + v_x^{g*}(k) \cdot \Delta k \\ v_x^{g*}(k+1) &= v_x^{g*}(k) + a_{comf} \cdot \Delta k \end{aligned} \quad (11)$$

a_{comf} denotes comfortable acceleration, which is the constant acceleration input, Δk is the discrete prediction time step. Let γ_P^i be a binary variable with $\gamma_P^i \in \{1, 0\}$, denoting i 's decision to yield such that $\gamma_P^i = 1 := i$ decides to yield, and is defined as

$$\gamma_P^i = \begin{cases} 1, & \text{if } \exists g \in \mathbb{A}_P \ \& \ [x^i \geq X^l - r_a^S] \ \& \ [v_x^i \geq 5] \\ & \ \& \ [x_P^{g*} \geq X^l] \ \& \ [v_x^i - v_e^* \geq 0.5 \cdot v_x^i] \\ 0, & \text{otherwise} \end{cases} \quad (12)$$

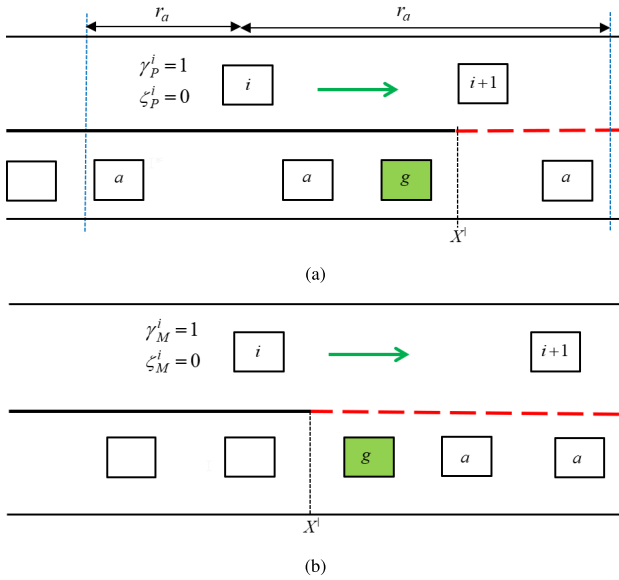


Fig. 2. Example illustration leader selection for yielding in the vicinity of highway merge (a) i (Predictive ADS) selects g from set of adjacent vehicles a 's (b) i (human driver) selects g from set of adjacent vehicles a 's.

where X^l is the start of the acceleration lane. This model includes four conditions: 1) the start of the acceleration lane should be within the detection range of i ; 2) $v_x^i \geq 5$ to prevent i from reaching a complete stop in the process of yielding; 3) g should be predicted to enter the acceleration lane, represented as $[x_p^{g*} \geq X^l]$; 4) yielding should not entail major loss of speed to i , represented as $v_x^i - v^e \geq 0.5 \cdot v_x^i$.

Thereafter, the prediction \mathbf{x}^{g*} is inspected to find the discrete prediction instance k^* when g encroaches the acceleration lane, i.e. $x_k^{g*} \geq X^l$. Let v_e^* be the corresponding predicted velocity, i.e. $v_e^* = v_{x,k^*}^{g*}$. The objective of the yielding control law is to regulate the v_x^i to achieve the safe spacing $s^i = s^0 + v_x^i \cdot t_d$ at the predicted moment of cut-in. Therefore, the acceleration to yield a_{YLD} in order to achieve this safety condition is derived as

$$a_{YLD} = \frac{x^g(k^*) - x^i(0) - s(0) - l - v_x^i(0)(k^* \Delta k + t_d)}{0.5(k^* \Delta k)^2 + t_d k^* \Delta k} \quad (13)$$

By inserting the tactical commands γ_P^i and ζ_P^i , and a_{YLD} in the control law, the acceleration with predictive cut-in handling a_{PH}^i is modelled as

$$a_{PH}^i = \min \left\{ a_{ACC}(i+1), \zeta_P^i \cdot a_{ACC}(c), [\gamma_P^i - \zeta_P^i] \cdot a_{YLD}(g) \right\} \quad (14)$$

The acceleration model of predictive cut-in handling implies that if an adjacent vehicle cuts in, the Predictive-ADS would treat the merging vehicle as its new leader and the yielding behavior will be blocked.

3) *Model With Manual Cut-In Handling*: The manual cut-in handling is modeled based on two assumptions: 1) the human driver can detect a cut-in at any distance, $r_a^M = \infty$, hence $\zeta_M^i = \zeta^i$; 2) the human driver will yield to an adjacent vehicle on the acceleration lane. The second assumption is based on

empirical observations that human drivers yield to adjacent vehicles before a cut-in [40].

The human driver considers a set of vehicles $\mathbb{A}_M \subset \mathbb{O}$ such that $A_M^i : a \in \mathbb{A}_M | x^a \geq X^l$. Thereafter it selects a vehicle g from \mathbb{A}_M , such that $g \in \mathbb{A}_M | x^{i+1} \geq x^g \geq x^i$ and $s(i, d) = \min \{s(i, g) | a \in \mathbb{A}_M\}$. This rule prescribes that g should be i 's nearest adjacent vehicle which is behind $i+1$. Figure 2(b) illustrates the selection of g by human driver in a traffic situation. Let the binary variable γ_M^i denote i 's decision to yield with $\gamma_M^i \in \{1, 0\}$ such that $\gamma_M^i = 1 := i$ decides to yield and is defined as

$$\gamma_M^i = \begin{cases} 1, & \text{if } \exists g \in \mathbb{A}_M \text{ and } v_x^i \geq 5 \\ 0, & \text{otherwise} \end{cases} \quad (15)$$

By inserting the tactical commands γ_M^i and ζ_M^i to the control law, the acceleration with manual cut-in handling a_{MH}^i is modeled as

$$a_{MH}^i = \min \left\{ a_{IDM}(i+1), \zeta_M^i \cdot a_{IDM}(c), [\gamma_M^i - \zeta_M^i] \max \{a_{IDM}(g), a_{gap}\} \right\} \quad (16)$$

where a_{gap} is the minimum acceleration that an HV would apply in order to yield.

C. Model for Lane-Changing

The lane change process of HV is modeled as two steps: lane-changing decision and lane-changing execution.

1) *Lane Change Decision*: We formulate the manual lane-changing decision by the model: Minimising Overall Braking Induced by Lane changes (MOBIL) [41]. This model has been widely used to describe the lane-changing decision of HVs. MOBIL specifies the manual lane-changing decision as a set of compact rules, under the assumption that the human driver can estimate the acceleration of its neighboring vehicle (HV or ADS-equipped vehicle). It derives the utility and risk of a lane change from the acceleration model of three vehicles: the lane-changing vehicle (c), following vehicle in the current lane (r) and potential follower in the target lane (f). In this model, the utility of a lane change is defined as

$$U = \tilde{a}^c - a^c + p \left[\tilde{a}^f - a^f + \tilde{a}^r - a^r \right] \quad (17)$$

where a^c is the acceleration of c in the current lane and \tilde{a}^c is its acceleration after the prospective lane change. Similarly, the current and prospective accelerations of the original follower o and potential follower f are included in the model, and p is a model parameter representing the politeness of c . The lane-changing decision is modeled as a dynamic variable by the following rule,

$$\begin{aligned} \zeta(t) &= \begin{cases} +1 : \tilde{a}_{right}^f(t) \geq b_{safe} \ \& \ U_{right} > \Delta a_{th} \ \& \ U_{right} \geq U_{left} \\ -1 : \tilde{a}_{left}^f(t) \geq b_{safe} \ \& \ U_{left} > \Delta a_{th} \ \& \ U_{left} > U_{right} \\ 0 : \text{otherwise} \end{cases} \end{aligned} \quad (18)$$

a_{th} the threshold of overall acceleration gain. Note that $\xi(t)$ is a dynamic variable which can be modified during the lane-changing. Thereby, this formulation allows a lane change to be aborted if the prospective acceleration of the follower is beyond the safe limit, b_{safe} [36].

2) *Lane-Changing Re-Planning and Trajectory*: The lane-changing trajectory is modeled as time-based polynomial function that is dynamically updated [36]. Polynomial functions have been widely used to model empirical lane-changing trajectories [42] and as reference paths for Automated steering control systems for lane-changing [43]. The two polynomial functions representing the independent time series of lateral and longitudinal position during the lane-changing is given as

$$\begin{aligned} y(t) &= a_5 t^5 + a_4 t^4 + a_3 t^3 + a_2 t^2 + a_1 t + a_0 \\ x(t) &= b_2 t^2 + b_1 t + b_0 \end{aligned} \quad (19)$$

The above functions include nine unknown coefficients which can be determined by solving for the boundary conditions of the lane change process. Accordingly, all these unknowns can be formulated as a function of longitudinal acceleration, a_x^c ; lane-changing duration, D ; and target lateral displacement by lane change, approximated by the lane width, W . During the lane change, c follows the preceding vehicles in the original l and target lanes p , and $a_x^c = \min\{a_{IDM}(p), a_{IDM}(l)\}$. The duration of each lane-changing is estimated at the start of the maneuver by the model of [44]. This model estimates D as a function of traffic density and relative kinematics of ambient vehicles, such as spacing and relative velocity. The lane change duration given by the model is not inherently bounded. Therefore, in the simulations, the range of D is bounded as $2 \leq D \leq 8$ within the empirically observed values [40]. The lane-changing is initiated when $\xi(t) = \pm 1$. In case of a lane change abortion, i.e if $\xi(t) = 0$ during an ongoing lane change execution, the target lateral displacement is updated to bring the vehicle back to its original lane. If the lane changer is a merging vehicle, it will decelerate when moving forward in the acceleration lane after the lane change abortion and evaluate the next available gap. It will come to standstill if it fails to find an acceptable gap before the end of the acceleration lane.

III. SAFETY METRICS

This section presents a set of SMOs to comprehensively evaluate the cut-in maneuvers covering aspects such as crash likelihood, crash severity and risk dynamics. The selected safety metrics are Post Encroachment Time (PET) to identify the conflicts with neighboring vehicles, Delta-V as a crash severity estimate, and Probabilistic Driving Risk Field strength that measures the driving risk as a dynamic variable combining both crash likelihood and crash severity.

PET represents the temporal proximity to a crash and has been used as a measure for crash likelihood. PET is the time elapsed between the two vehicles passing a predefined location on the road stretch. During a cut-in, PET is measured between the cut-in vehicle and neighboring vehicles $n \in \{f, r, p, t\}$ as shown in Figure 6, where f denotes the follower in the

target lane; r denotes follower in the current lane; p denotes preceding vehicle in the current lane; and t denotes preceding vehicle in target lane. This results in four measurements. We adopt the method proposed in a previous study [45] to measure PET of a cut-in. Accordingly, the PET with respect to any n is measured based on the x coordinate of the location at which the closest corner of c crosses the lane boundary [45]. In this study, cut-ins with PET < 0.5 s are labelled as a conflict [20].

Delta-V is a widely used measure of crash severity, i.e. consequences of the crash in terms of property damage. It is defined as the change in velocity of cut-in vehicle c (See Figure 6) between its pre-crash and post-crash trajectories if it crashes with a neighbor n under consideration [46]. Similar to PET, Delta-V is measured between the cut-in vehicle, and neighboring vehicles n , resulting in four measurements. Among the four measurements, the maximum Delta-V is used as the representative of the maneuver. Delta-V is defined for an inelastic crash between c and n , i.e. they stick together after collision and that they have the same mass. Assuming that n does not move laterally at the time of measurement, Delta-V can be defined as

$$\Delta V^c = \sqrt{\left(\frac{v_x^n - v_x^c}{2}\right)^2 + \left(\frac{v_y^c}{2}\right)^2} \quad (20)$$

Field theory-based safety metrics represents the driving risk as dynamic variable combining crash likelihood and severity [20]. Such a measure would allow a straightforward comparison of maneuver safety. Based on field-theory, we proposed an approach to assess the driving risk: the risk taken by a vehicle as a result of its interaction with adjacent entities [37]. This approach-Probabilistic Driving Risk Field (PDRF)-can describe the driving risk in interaction with both vehicles and road-side barriers. In this study, we employ this approach solely to quantify the driving risk with respect to f . This approach treats f as an obstacle to c , and models f as a finite scalar risk field formulated in the predicted configuration space of the c . Thereby, the driving risk of c at any given moment is the value of the risk field at the position of its centre of mass.

$$R^c(f) = \frac{M^c \cdot |\mathbf{v}^c - \mathbf{v}^f|^2 \cdot P(f, c)}{8} \quad (21)$$

This risk field is formulated as the product of expected crash energy and the collision probability. The term $\frac{M^c \cdot |\mathbf{v}^c - \mathbf{v}^f|^2}{8}$, depicts the expected crash energy if c collides inelastically with f . The second term $P(f, c)$ describes the crash probability between the c and f . The possible states of f at a future time step is estimated from its acceleration distribution. $P(f, c)$ depicts the probability of overlap in the predicted position of c over the possible positions of f at the future time step, which is set as 3 s in our analysis.

IV. CASE STUDY AND RESULTS

In this section, we present the simulation experiments wherein the ADS and HV models are numerically implemented as time-discrete simulations. The objective of these experiments is to compare the impacts of ADS cut-in handling

approaches on the safety and characteristics of HV's lane changes. We simulate a two-lane highway section of 7.3 km with an on-ramp. The on-ramp merges with the highway through an acceleration lane of 300 m starting from 5 km. This road geometry allows controlling the number of cut-ins (merges) disturbing the main-lane traffic. The simulation framework assembling several behavioral component models as described in Section II was implemented in Matlab [36].

We select two primary input parameters. First, the traffic demand on the on-ramp was set as 250 veh/hr/lane (representing low disturbance) and 750 veh/hr/lane (representing high disturbance) based on empirical observations on Dutch freeways [47]. The two demands represent different levels of disturbances and do not trigger traffic breakdown, after which complex congestion wave formation and propagation dominate the behaviors of vehicles and drivers tend to override ADS systems [21]. Second, the share of ADS-equipped vehicles on the main-lane traffic, set as 0% (reference scenario without ADS-equipped vehicle in traffic), 10% (approximately the current deployment rate of such systems in Europe) [48], 30%, 50% and 90% representing different levels of the mix. Thereby, reactive and predictive cut-in handling approaches are evaluated in two sets of traffic scenarios (varying in the combination of the two input parameters). The resulting scenario matrix consists of 18 scenarios. To improve the statistical reliability of the results, we perform 10 replications of each scenario. The simulations are randomized in terms of the vehicle generation and the desired velocity of HV. To ensure the comparability of the results across the scenarios, the values all the driving model parameters (See Table II) is fixed across all the simulations. Each scenario is simulated for 30 minutes at a discrete-time step of 0.1 s.

A. Characteristics of Lane Changes

We evaluate the change in characteristics of lane changes as an effect of the increasing presence of ADS-equipped vehicles. Figure 3 plots the spatial distribution of successful lane changes performed by humans under scenarios with an increasing penetration rate of ADS-equipped vehicle. In all the plots, the distribution peaks in the vicinity of merging section (5000 - 5300 m), where on-ramp vehicles merge into the main lane. It can be seen that HV's perform more lane changes in mixed traffic (See Figure 3). In traffic mixed with Reactive ADS, the lane change frequency at the downstream end of the merging section is higher than at the upstream end. This indicates an increase in the number of late merges due to the lack of cooperation by Reactive ADS (See Figure 3(a) and (c)). In contrast, such a disparity is not observed in the presence of Predictive ADS; the lane changes occur throughout the merging section (See Figure 3(b) and (d)).

Figure 4 plots the average velocity at the start of a lane change. The lane changing velocity consistently drops with an increasing presence of reactive ADS. As most of the lane changes are merging maneuvers, the velocity reduces as vehicles queue up at the on-ramp dead-end, implying an increase in difficulty to find a safe merging gap. In contrast, Predictive ADSs increase the lane-changing velocity at low on-ramp demand. The early yielding by ADS enables smooth

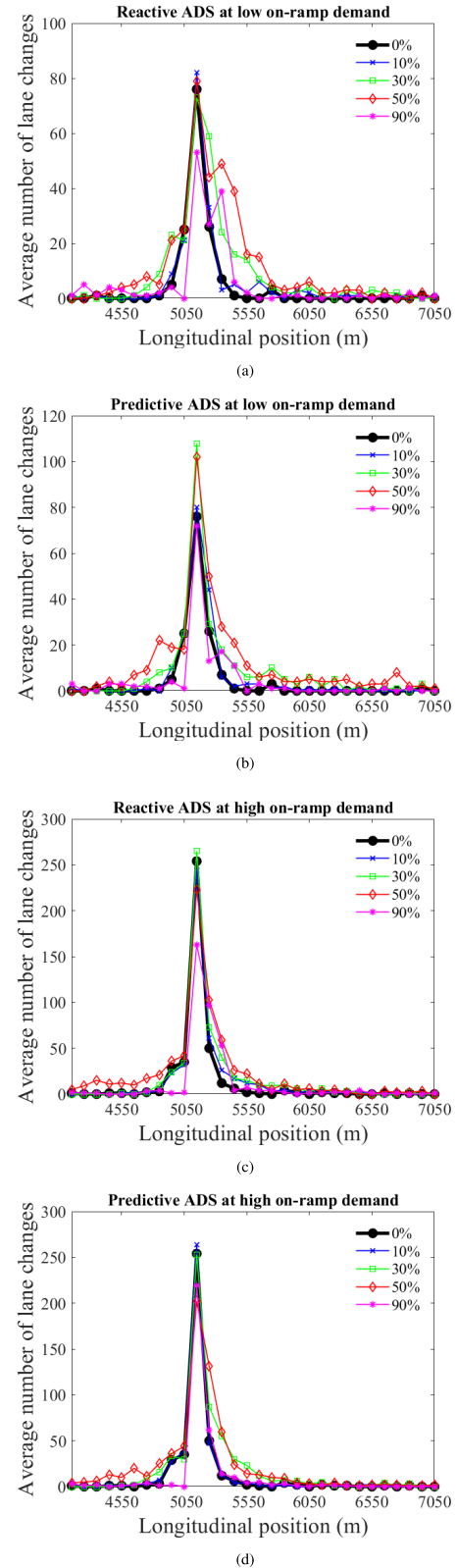


Fig. 3. Effects of ADS penetration on the spatial distribution of lane changes at low on-ramp demand (a),(b) and high on-ramp demand (c),(d).

merging of the on-ramp vehicle. At the 90% penetration rate, the difference in the effects of reactive and predictive ADS, as observed by lane change velocity becomes prominent. Interestingly, at 50% penetration rate, the effects (as observed

TABLE II
PARAMETER VALUES IN THE SIMULATION EXPERIMENTS

Parameter (description)	Value	Parameter (description)	Value
\bar{a} (IDM maximum acceleration)	1 m/s ²	K_1 (ACC parameter)	0.1 1/s ²
b (IDM comfortable braking)	1.5 m/s ²	K_2 (ACC parameter)	5.4 1/s
v^{max} (IDM maximum speed)	160 km/hr	K_3 (ACC parameter)	0.12 1/s ²
v_d (desired velocity)	108 km/hr	Q (ACC parameter)	1
t_d (desired time headway)	1.2 s	J (ACC parameter)	100 m
s_0 (IDM minimum space gap)	2 m	X^1 (start of acceleration lane)	5000 m
m (Vehicle mass)	1000 kg	w (Vehicle width)	2 m
W (Lane width)	3.5 m	l (Vehicle length)	5 m
b_{safe} (safe braking limit)	4 m/s ²	a_{min} (maximum braking)	-9 m/s ²
p (MOBIL politeness parameter)	0.5	a_{max} (maximum acceleration)	3 m/s ²
Δa_{th} (MOBIL acceleration threshold)	0.5	Simulation time step	0.1 s

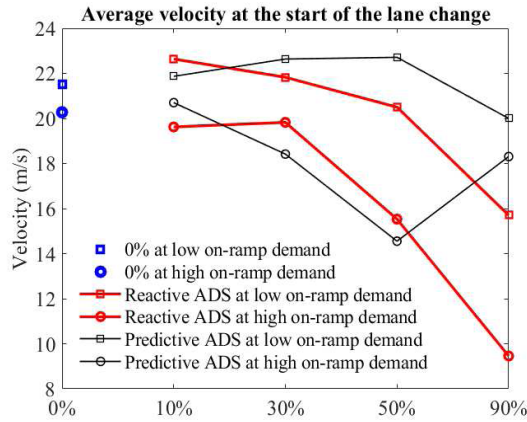


Fig. 4. Effects of ADS penetration rate on the velocity at the start of lane change.

by the lane change velocity) are comparable between the two cut-in handling approach. The reason is that, in 50% mixed traffic, the number of lane changes in the vicinity of the merge is relatively higher (see Figure 3 (c) and (d)), creating congestion on the main lanes. Since the predictive control does not function in a velocity of < 5 m/s, the effect of Predictive ADSs on the merging vehicles is similar to that of Reactive ADSs at this penetration rate.

B. Aborted Lane Changes

Figure 5 describes the effect of ADS penetration rate on the number of aborted (unsuccessful) lane changes with high on-ramp demand. It can be seen that the aborted lane changes steadily increase with the presence of Reactive ADS. The Reactive ADS cannot respond to the cut-in vehicle during the first half of the cut-in maneuver. This creates risky situations, i.e. $\tilde{a}^f(t) < b_{safe}$ in Equation 18, causing c to abort the lane change. On the contrary, aborted lane changes are occasional (< 1) in traffic scenarios with predictive ADS-equipped

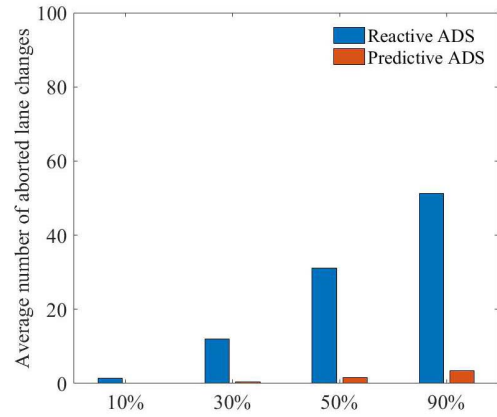


Fig. 5. Effects of ADS penetration rate on the number of aborted lane changes at high on-ramp demands.

vehicles, irrespective of their market penetration rate and on-ramp demand. The predictive ADS begin to respond to cut-in at least by the start of the maneuver, and therefore risky situations are avoided. Similarly, we observed aborted lane changes with low on-ramp demand in traffic consisting of Reactive ADS: a maximum of six aborted lane changes at 90% penetration rate of Reactive ADS.

C. Conflicts With Neighboring Vehicles

We evaluate the conflicts between c and any of its neighbors $n \in \{f, r, p, t\}$ as shown in Figure 6. Figure 7 describes the effects of the increasing penetration rate of ADS-equipped vehicle on lane-change conflicts. The number of conflicts increases with the market penetration rate of ADS-equipped vehicle irrespective of the cut-in handling approach. It can be seen that Predictive ADS results in fewer conflicts than Reactive ADS. The highest number of conflicts appears between the c and f , following vehicle in the target lane that is

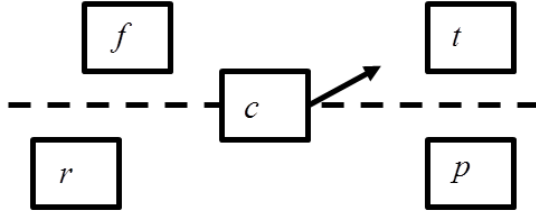


Fig. 6. Notations for the vehicles in the vicinity of the lane changer c .

handling the cut in, and with an increasing market penetration rate, it is more likely that f is an ADS-equipped vehicle. ADS-equipped vehicle applies a relatively milder acceleration than HV according to their respective control laws, which shortens the PET of the maneuver. Therefore the behavioral distinction of ADS-equipped vehicle poorly reflects in the PET metric. In scenarios with high on-ramp demand, the higher number of conflicts appears between the c - r , and c - p . High demand induces queuing in the on-ramp lane, and vehicles are close to each other, resulting in shorter PET. This is in line with the observed drop in lane change velocity (Figure 4).

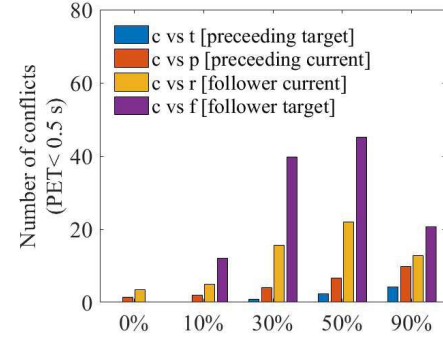
D. Expected Severity of Crashes

Figure 8 describes the effects of increasing the ADS-equipped vehicle share on the average maximum Delta-V. It can be seen that the impact on the expected crash severity (as estimated by Delta-V) is marginal, except in 90% penetration rate at low on-ramp demand. With lower disturbance from the on-ramp, the main-lane traffic flows at higher speed, resulting in larger Delta-V during cut-in. Delta-V related to Predictive ADS is lower than that of Reactive ADS. The Predictive ADS yields earlier allowing it to lower the approach speed.

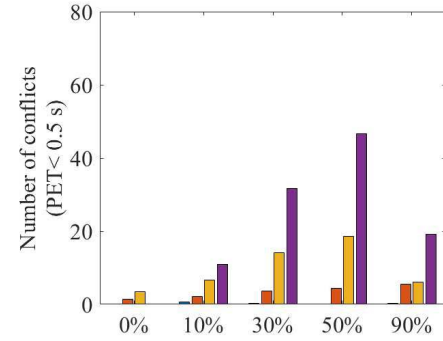
E. Driving Risk During Cut-In

The PDRF incorporates both the crash severity and crash probability and thereby allows straightforward risk comparison. To compare the specific effects of Reactive and Predictive control, we solely analyze cut-ins ahead of ADS-equipped vehicle. Figure 9 describes the effects of increasing ADS-equipped vehicle share on the average maximum driving risk as estimated by PDRF strength. It can be seen that cut-ins involving Predictive ADS are consistently at a lower risk than those involving Reactive ADS. Besides, the magnitude of risk with cut-in is expected to steadily increase with the share of Reactive ADS in traffic, and the variation of risk estimate increases with the penetration rate, suggesting the increasing variability in the risk level of conflicts. In contrast, the magnitude of risk and its variability in cut-ins involving Predictive ADS remain marginal throughout all scenarios.

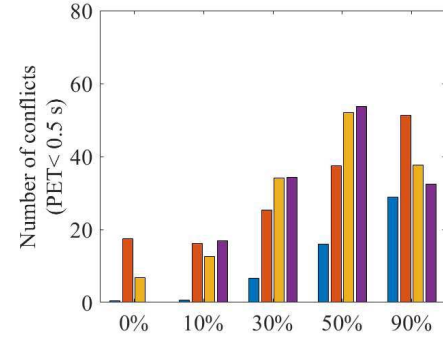
Figure 10 describes the effects of ADS on the risk dynamics during an average cut-in. When the traffic is mixed with Reactive ADS, the driving risk peaks halfway during the maneuver, and drops thereafter. This effect can be due to two combining factors: reactive ADS-equipped vehicles cannot respond to the



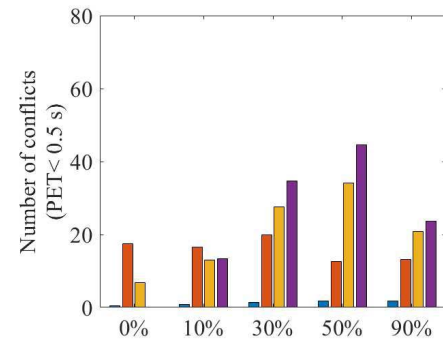
(a) Reactive ADS at low on-ramp demand



(b) Predictive ADS at low on-ramp demand



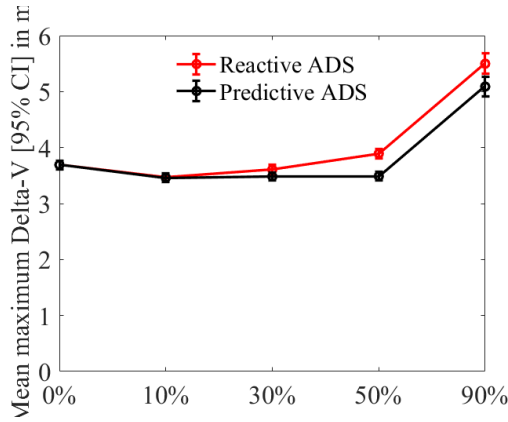
(c) Reactive ADS at high on-ramp demand



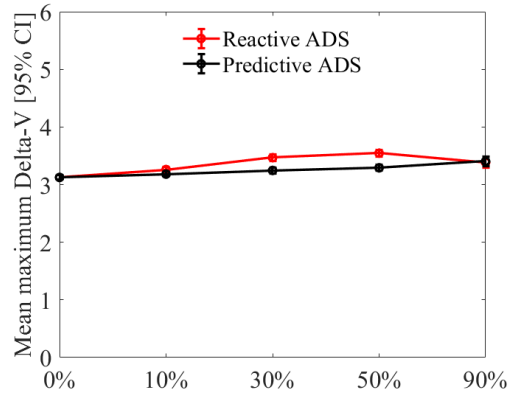
(d) Predictive ADS at high on-ramp demand

Fig. 7. Effects of ADS penetration rate on the frequency of conflicts between the c (cut-in vehicle) and each of its neighbors $n \in \{f, r, p, t\}$ at low on-ramp demand (a),(c) and high on-ramp demand (b),(d).

cut-in vehicle during the first half of the cut-in maneuver, causing a steep rise in crash probability; the lateral velocity of the lane-changer is highest when halfway through the



(a) Low on-ramp demand



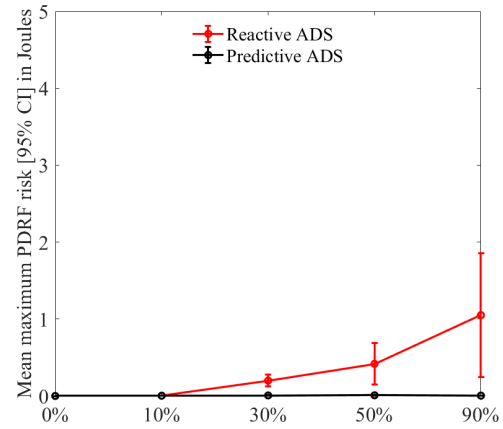
(b) High on-ramp demand

Fig. 8. Effects of ADS penetration rate on mean Delta-V at low (a) and high on-ramp demands (b).

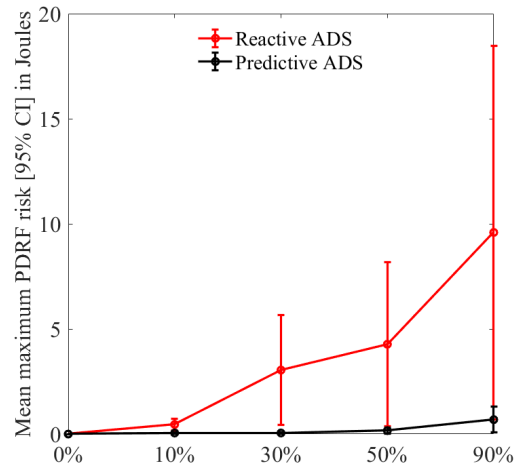
maneuver, implying a peak of expected crash severity. During the second half of cut-in, the follower (Reactive ADS) begins to respond preventing a further rise in risk. In contrast, when the traffic is mixed with predictive ADS-equipped vehicle, there is no such intermediate peak in driving risk; instead, the driving risk remains marginal throughout the maneuver. Besides, it can be seen from Figure 10 that the magnitude of the risk peak increases steadily with the penetration rate of Reactive ADS.

V. SENSITIVITY ANALYSIS

In this section we discuss the implications of the parameter values and model choice on the results. The length of the acceleration lane was set to 300 m in the scenario simulations. To evaluate the implication of this setting, we simulated homogeneous HV traffic under high on-ramp demand with a longer acceleration lane of 500 m. Acceleration lane lengths are set as 300 and 500 meters according to design practices in Europe and the Netherlands [49], [50]. In this scenario, we observe that the expected crash severity drops to 2.11 m/s (from 3.12 m/s), whereas the number of conflicts increases to 39 (from 25). The increase in the number of conflicts is a direct effect of increasing the road space available for merging. In traffic mixed with Reactive ADS, a larger acceleration lane



(a) Low on-ramp demand



(b) High on-ramp demand

Fig. 9. Mean maximum PDRF risk with low on-ramp demand (a) and high on-ramp demand (b).

length can have a positive effect on safety. For instance, in 50% mix of Reactive ADS at high on-ramp demand, the instances of lane change abortion are reduced to 10 from 30 (See Figure 5), and average maximum Delta-V reduces by 0.3 m/s.

The sensing range of Predictive ADS was set to 200 m. We did not find a considerable improvement in the safety performance of Predictive ADS, when the sensing range is increased to 300 m, for instance the average maximum Delta-V reduced marginally by 0.1 m/s.

The longitudinal acceleration control of an ADS-equipped vehicle was modeled by a deterministic ACC law [24], and HV was modeled by IDM with the desired velocity as a stochastic parameter. Besides, ADS-equipped vehicle does not change lane, whereas HV can change lane. To check if our comparative findings hold even when the effects of distinct acceleration and lane change models are excluded, we analyzed simulations in which longitudinal control of all the vehicles was modeled by IDM [39] (with a fixed desired velocity) and lane-changing decision by MOBIL. We find that the above findings comparing the reactive and predictive ADS hold under such modeling assumptions as well.

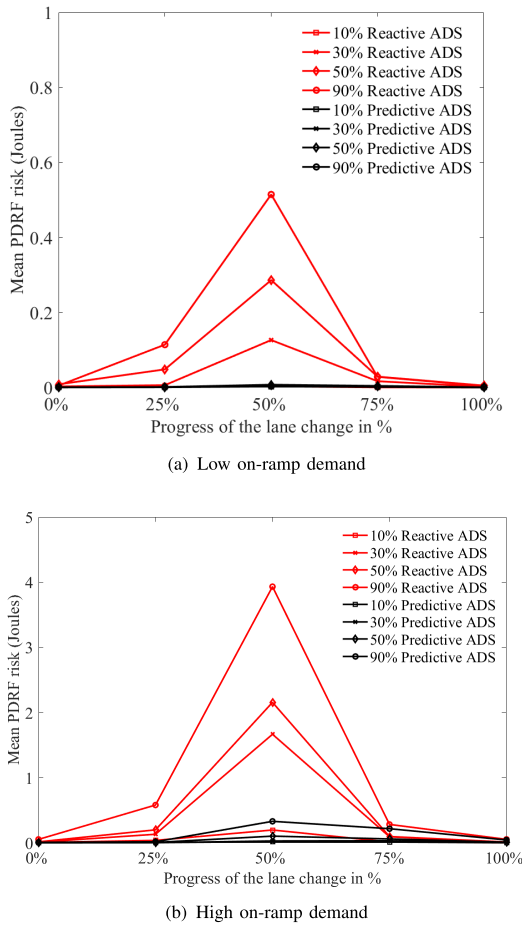


Fig. 10. Evolution of risk during lane-changing in scenarios with ADS at low (a) and high on-ramp demands (b).

In traffic scenarios comprising of vehicles with reactive control, we observed 23 (at low on-ramp demand) and 149 (at high on-ramp demand) instances of aborted lane changes, but no aborted lane changes were observed in traffic with predictive control. With low on-ramp demand, in traffic scenarios comprising of vehicles with reactive control, the maximum Delta-V was larger (5.2 m/s) than that of traffic with predictive control (4.4 m/s). The reactive control resulted in average 62.2 (low on-ramp demand) and 411.3 (high on-ramp demand) conflicts, which is considerably larger than 3.7 (low on-ramp demand) and 6.3 (high on-ramp demand) with the predictive control.

To exclude the effects of the lane-changing decision model, we analyzed simulations of an IDM controlled traffic fleet with high on-ramp demand. In this case, MOBIL is deactivated and vehicles on the main lane do not change lane. The results further strengthen our finding that predictive control is safer than the reactive one. In traffic scenarios comprising of vehicles with reactive control, we observed 90 (in high on-ramp demand) instances of aborted lane changes, but no aborted lane changes were observed in traffic with predictive control. The reactive control resulted in 358 conflicts, in contrast, we did not observe any conflict in traffic with predictive control. Similarly, in traffic scenarios comprising of vehicles with reactive control, the maximum Delta-V was larger (5.1 m/s) than that of traffic with predictive control (2.5 m/s).

Models in this study strongly idealize the behavior of sensors and actuators in the ADS. Similarly, a simple rule-based algorithm was deployed to model the prediction logic of the ADS. Under these assumptions, our results suggest that even a simple prediction scheme could significantly outperform reactive approaches in terms of traffic safety. However, the quantitative accuracy of the results can be improved by relaxing these assumptions and rigorously modeling sophisticated prediction algorithms or other approaches in reactive ADS to improve the robustness of cut-in handling [51].

Another assumption underlying the lane change decision model is that human drivers can estimate the acceleration gain for the adjacent vehicle (human or equipped), as a consequence of lane changes [41]. This assumption is not realistic in mixed traffic scenarios with low ADS market penetration, when the human drivers might not be familiar with behavior of ADS-equipped vehicle. However, we do not expect any influence on the comparative findings, as the assumption applies to both sets of mixed traffic simulations.

VI. CONCLUSION AND FUTURE WORK

It is well known that ADS equipped vehicles can impact the longitudinal driving behavior of the non-equipped vehicles and the collective traffic flow properties. Our results suggest the longitudinal functionalities of the ADS can impact the lateral maneuvers of adjacent vehicles (human-driven vehicles in this study) as well. We find that the presence of ADS-equipped vehicles in traffic could alter the spatial distribution of lane change events in the vicinity of the merging section; Reactive ADS could increase the difficulty to safely merge onto the highway, thereby increasing the level of congestion in the on-ramp; and that Reactive ADS could increase the instances of unsuccessful lane changes.

We find that approaches employed by ADS-equipped vehicles to handle a cut-in can impact traffic safety at a highway discontinuity. The predictive control is the key functionality to improve safety with cut-ins. The predictive control employing a simple rule-based decision provides a safer interaction than reactive control. These two approaches yield distinct risk dynamics during a cut-in. When a vehicle cuts in ahead of Reactive ADS, the risk peaks approximately halfway through the maneuver. This is also reflected by the instances of lane change abortions. In contrast, the prediction functionality maintains the risk marginal throughout the encounter. Regarding the variation of safety impact with the market penetration rate of ADS equipped vehicles, we find that the negative effects of Reactive ADS become prominent when the penetration rate is greater than 10% and grows strongly with penetration rate. The level of traffic safety is approximately unaffected by the increasing share of Predictive ADS.

Our results highlight the potential of simulation-based safety assessment in this regard. Our future efforts will be focussed on analysing the safety impacts of a specific ADS feature that is already deployed in passenger vehicles and to provide more concrete estimates such as expected crash rate and related proportion of fatalities. Moreover, the relationship between aborted lane changes and length of acceleration lanes deserves dedicated attention, including conditions and model

parameters leading to aborted lane changes, such as the length of the acceleration lane, cooperative behavior of ADS-equipped vehicles and HVs in lane change events.

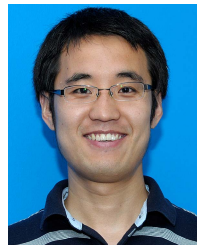
REFERENCES

- [1] SAE On-Road Automated Vehicle Standards Committee. "Taxonomy and definitions for terms related to on-road motor vehicles J," SAE Tech. Paper 3016:2014, 2018, pp. 1–16.
- [2] C.-Y. Chan, "Advancements, prospects, and impacts of automated driving systems," *Int. J. Transp. Sci. Technol.*, vol. 6, no. 3, pp. 208–216, Sep. 2017.
- [3] M. Sivak and B. Schoettle, "Road safety with self-driving vehicles: General limitations and road sharing with conventional vehicles," Univ. Michigan Transp. Res. Inst., Ann Arbor, Tech. Rep. UMTRI-2015-2, Jan. 2015.
- [4] L. Yue, M. Abdel-Aty, Y. Wu, and L. Wang, "Assessment of the safety benefits of vehicles' advanced driver assistance, connectivity and low level automation systems," *Accident Anal. Prevention*, vol. 117, pp. 55–64, Aug. 2018.
- [5] J. B. Cicchino, "Effectiveness of forward collision warning and autonomous emergency braking systems in reducing front-to-rear crash rates," *Accident Anal. Prevention*, vol. 99, pp. 142–152, Feb. 2017.
- [6] M. Perez *et al.*, "Advanced crash avoidance technologies (ACAT) program—final report of the GM-VTTI backing crash countermeasures project," U.S. Dept. Transp. Nat. Highway Traffic Saf. Admin., Tech. Rep. DOT HS 811 452, 2011.
- [7] D. D. Salvucci and A. Liu, "The time course of a lane change: Driver control and eye-movement behavior," *Transp. Res. F, Traffic Psychol. Behav.*, vol. 5, no. 2, pp. 123–132, Jun. 2002.
- [8] M. S. Rahman, M. Abdel-Aty, J. Lee, and M. H. Rahman, "Safety benefits of arterials' crash risk under connected and automated vehicles," *Transp. Res. C, Emerg. Technol.*, vol. 100, pp. 354–371, Mar. 2019.
- [9] C. Letter and L. Eleftheriadou, "Efficient control of fully automated connected vehicles at freeway merge segments," *Transp. Res. C, Emerg. Technol.*, vol. 80, pp. 190–205, Jul. 2017.
- [10] A. Papadoulis, M. Qudus, and M. Imprialou, "Evaluating the safety impact of connected and autonomous vehicles on motorways," *Accident Anal. Prevention*, vol. 124, pp. 12–22, Mar. 2019.
- [11] C. Menendez-Romero, M. Sezer, F. Winkler, C. Dornhege, and W. Burgard, "Courtesy behavior for highly automated vehicles on highway interchanges," in *Proc. IEEE Intell. Vehicles Symp. (IV)*, Jun. 2018, pp. 943–948.
- [12] Y. Tu, W. Wang, Y. Li, C. Xu, T. Xu, and X. Li, "Longitudinal safety impacts of cooperative adaptive cruise control vehicle's degradation," *J. Saf. Res.*, vol. 69, pp. 177–192, Jun. 2019.
- [13] E. Jeong and C. Oh, "Evaluating the effectiveness of active vehicle safety systems," *Accident Anal. Prevention*, vol. 100, pp. 85–96, Mar. 2017.
- [14] M. Bahram, Z. Ghandeharioun, P. Zahn, M. Baur, W. Huber, and F. Busch, "Microscopic traffic simulation based evaluation of highly automated driving on highways," in *Proc. ITSC*, Oct. 2014, pp. 1752–1757.
- [15] D. Zhao *et al.*, "Accelerated evaluation of automated vehicles safety in lane-change scenarios based on importance sampling techniques," *IEEE Trans. Intell. Transp. Syst.*, vol. 18, no. 3, pp. 595–607, Mar. 2017.
- [16] M. S. Rahman, M. Abdel-Aty, L. Wang, and J. Lee, "Understanding the highway safety benefits of different approaches of connected vehicles in reduced visibility conditions," *Transp. Res. Rec. J. Transp. Res. Board*, vol. 2672, no. 19, pp. 91–101, Dec. 2018.
- [17] M. Guériau, R. Billot, N.-E. El Faouzi, J. Monteil, F. Armetta, and S. Hassas, "How to assess the benefits of connected vehicles? A simulation framework for the design of cooperative traffic management strategies," *Transp. Res. C, Emerg. Technol.*, vol. 67, pp. 266–279, Jun. 2016.
- [18] S. Wang and Z. Li, "Exploring the mechanism of crashes with automated vehicles using statistical modeling approaches," *PLoS ONE*, vol. 14, no. 3, 2019, Art. no. e0214550.
- [19] H. Park, C. S. Bhamidipati, and B. L. Smith, "Development and evaluation of enhanced intellidrive-enabled lane changing advisory algorithm to address freeway merge conflict," *Transp. Res. Rec. J. Transp. Res. Board*, vol. 2243, no. 1, pp. 146–157, 2011.
- [20] F. A. Mullakkal-Babu, M. Wang, H. Farah, B. van Arem, and R. Happee, "Comparative assessment of safety indicators for vehicle trajectories on highway," *Transp. Res. Rec.*, vol. 2659, no. 1, pp. 127–136, 2017.
- [21] L. Xiao, M. Wang, W. Schakel, and B. van Arem, "Unravelling effects of cooperative adaptive cruise control deactivation on traffic flow characteristics at merging bottlenecks," *Transp. Res. C, Emerg. Technol.*, vol. 96, pp. 380–397, Nov. 2018, [Online]. Available: <http://www.sciencedirect.com/science/article/pii/S0968090X1830528X>
- [22] W. G. Najm, J. D. Smith, and M. Yanagisawa, "Pre-crash scenario typology for crash avoidance research," NHTSA, Nat. Highway Traffic Saf. Admin., Washington, DC, USA, Tech. Rep. DOT HS 810 767, 2007.
- [23] S. Moon, I. Moon, and K. Yi, "Design, tuning, and evaluation of a full-range adaptive cruise control system with collision avoidance," *Control Eng. Pract.*, vol. 17, no. 4, pp. 442–455, Apr. 2009.
- [24] F. A. Mullakkal-Babu, M. Wang, B. van Arem, and R. Happee, "Design and analysis of full range adaptive cruise control with integrated collision avoidance strategy," in *Proc. IEEE 19th Int. Conf. Intell. Transp. Syst. (ITSC)*, Rio de Janeiro, Brazil, Nov. 2016, pp. 308–315.
- [25] A. F. L. Larsson, K. Kircher, and J. A. Hultgren, "Learning from experience: Familiarity with ACC and responding to a cut-in situation in automated driving," *Transp. Res. F, Traffic Psychol. Behav.*, vol. 27, pp. 229–237, Nov. 2014.
- [26] W. Ko and D. E. Chang, "Cooperative adaptive cruise control using turn signal for smooth and safe Cut-In," in *Proc. 18th Int. Conf. Control, Autom. Syst. (ICCAS)*, Oct. 2018, pp. 807–812.
- [27] A. Carvalho, A. Williams, S. Lefevre, and F. Borrelli, "Autonomous cruise control with cut-in target vehicle detection," in *Proc. 13th Int. Symp. Adv. Vehicle Control*, 2016, pp. 93–99.
- [28] T. Rehder, A. Koenig, M. Goehl, L. Louis, and D. Schramm, "Lane change intention awareness for assisted and automated driving on highways," *IEEE Trans. Intell. Vehicles*, vol. 4, no. 2, pp. 265–276, Jun. 2019.
- [29] J. Wei, J. M. Dolan, and B. Litkouhi, "Autonomous vehicle social behavior for highway entrance ramp management," in *Proc. IEEE Intell. Vehicles Symp. (IV)*, Gold Coast, QLD, Australia, Jun. 2013, pp. 201–207.
- [30] J. Schlechtriemen, A. Wedel, J. Hillenbrand, G. Breuel, and K.-D. Kuhnert, "A lane change detection approach using feature ranking with maximized predictive power," in *Proc. IEEE Intell. Vehicles Symp.*, Dearborn, MI, USA, Jun. 2014, pp. 108–114.
- [31] L. C. Davis, "Effect of adaptive cruise control systems on mixed traffic flow near an on-ramp," *Phys. A, Stat. Mech. Appl.*, vol. 379, no. 1, pp. 274–290, Jun. 2007.
- [32] M. Bahram, A. Wolf, M. Aeberhard, and D. Wollherr, "A prediction-based reactive driving strategy for highly automated driving function on freeways," in *Proc. IEEE Intell. Vehicles Symp.*, Jun. 2014, pp. 400–406.
- [33] M. Bahram, A. Lawitzky, J. Friedrichs, M. Aeberhard, and D. Wollherr, "A game-theoretic approach to replanning-aware interactive scene prediction and planning," *IEEE Trans. Veh. Technol.*, vol. 65, no. 6, pp. 3981–3992, Jun. 2016.
- [34] M. Wang, S. P. Hoogendoorn, W. Daamen, B. van Arem, and R. Happee, "Game theoretic approach for predictive lane-changing and car-following control," *Transp. Res. C, Emerg. Technol.*, vol. 58, pp. 73–92, Sep. 2015.
- [35] P. A. Ioannou and M. Stefanovic, "Evaluation of ACC vehicles in mixed traffic: Lane change effects and sensitivity analysis," *IEEE Trans. Intell. Transp. Syst.*, vol. 6, no. 1, pp. 79–89, Mar. 2005.
- [36] F. A. Mullakkal-Babu, M. Wang, B. van Arem, B. Shyrokau, and R. Happee, "A hybrid submicroscopic-microscopic traffic flow simulation framework," *IEEE Trans. Intell. Transp. Syst.*, early access, May 6, 2020, doi: [10.1109/TITS.2020.2990376](https://doi.org/10.1109/TITS.2020.2990376).
- [37] F. A. Mullakkal-Babu, M. Wang, X. He, B. van Arem, and R. Happee, "Probabilistic field approach for motorway driving risk assessment," *Transp. Res. C, Emerg. Technol.*, vol. 118, Sep. 2020, Art. no. 102716.
- [38] J. Nilsson, P. Falcone, M. Ali, and J. Sjöberg, "Receding horizon maneuver generation for automated highway driving," *Control Eng. Pract.*, vol. 41, pp. 124–133, Aug. 2015.
- [39] M. Treiber, A. Hennecke, and D. Helbing, "Congested traffic states in empirical observations and microscopic simulations," *Phys. Rev. E, Stat. Phys. Plasmas Fluids Relat. Interdiscip. Top.*, vol. 62, no. 2, pp. 1805–1824, Aug. 2000.
- [40] Z. Zheng, S. Ahn, D. Chen, and J. Laval, "The effects of lane-changing on the immediate follower: Anticipation, relaxation, and change in driver characteristics," *Transp. Res. C, Emerg. Technol.*, vol. 26, pp. 367–379, Jan. 2013.

- [41] A. Kesting, M. Treiber, and D. Helbing, "General lane-changing model MOBIL for car-following models," *Transp. Res. Rec. J. Transp. Res. Board*, vol. 1999, no. 1, pp. 86–94, Jan. 2007.
- [42] Q. Wang, Z. Li, and L. Li, "Investigation of discretionary lane-change characteristics using next-generation simulation data sets," *J. Intell. Transp. Syst.*, vol. 18, no. 3, pp. 246–253, Jul. 2014.
- [43] Y. Luo, Y. Xiang, K. Cao, and K. Li, "A dynamic automated lane change maneuver based on vehicle-to-vehicle communication," *Transp. Res. C, Emerg. Technol.*, vol. 62, pp. 87–102, Jan. 2016.
- [44] T. Toledo and D. Zohar, "Modeling duration of lane changes," *Transp. Res. Rec. J. Transp. Res. Board*, vol. 1999, no. 1, pp. 71–78, Jan. 2007.
- [45] L. Zheng, K. Ismail, and X. Meng, "Freeway safety estimation using extreme value theory approaches: A comparative study," *Accident Anal. Prevention*, vol. 62, pp. 32–41, Jan. 2014.
- [46] S. G. Shelby, "Delta-V as a measure of traffic conflict severity," in *Proc. 3rd Int. Conf. Road Saf. Simulation*, Indianapolis, Brazil, 2011, pp. 14–16.
- [47] M. Wang, S. van Maarseveen, R. Happee, O. Tool, and B. van Arem, "Benefits and risks of truck platooning on freeway operations near entrance ramp," *Transp. Res. Rec. J. Transp. Res. Board*, vol. 2673, no. 8, pp. 588–602, Aug. 2019.
- [48] M. Kyriakidis, C. van de Weijer, B. van Arem, and R. Happee, "The deployment of advanced driver assistance systems in Europe," in *Proc. 22nd ITS World Congr.*, Bordeaux, France, 2015, pp. 1–19.
- [49] H. Ruyters, M. Slop, and F. Wegman, "Safety effects of road design standards," Citeseer, Leidschendam, The Netherlands, Tech. Rep. R-94-7, 1994.
- [50] A. van Beinum and F. Wegman, "Design guidelines for turbulence in traffic on dutch motorways," *Accident Anal. Prevention*, vol. 132, Nov. 2019, Art. no. 105285.
- [51] T. Xia, M. Yang, R. Yang, and C. Wang, "CyberC3: A prototype cybernetic transportation system for urban applications," *IEEE Trans. Intell. Transp. Syst.*, vol. 11, no. 1, pp. 142–152, Mar. 2010.



Freddy Antony Mullakkal-Babu received the bachelor's degree in civil engineering from the National Institute of Technology Calicut in 2011 and the master's degree in transportation systems engineering from the Indian Institute of Technology, Mumbai, in 2014. He is currently pursuing the Ph.D. degree with the Department of Transport and Planning, Delft University of Technology. His research interests include driver behavior modeling, traffic safety, and design and assessment of driving automation systems.



Meng Wang (Member, IEEE) received the bachelor's degree in civil engineering from Tsinghua University, in 2003, the M.Sc. degree in transportation engineering from the Research Institute of Highway, China, in 2006, and the Ph.D. degree in transport and planning from the Delft University of Technology, The Netherlands, in 2014. From 2014 to 2015, he was a Post-Doctoral Researcher with the Department of Biomechanical Engineering, Delft University of Technology. Since 2015, he has been an Assistant Professor (tenured in 2019) with the Department of Transport and Planning, Delft University of Technology. His research interests include driving behavior modeling, traffic flow, and control approaches for cooperative driving systems. He is also the Co-Director of the Electric and Automated Transport Laboratory, TU Delft. He is also an Associate Editor of IEEE TRANSACTIONS ON INTELLIGENT TRANSPORTATION SYSTEMS (ITS), *IET Intelligent Transport Systems (ITS)*, and *Transportmetrica B*.



Bart van Arem (Senior Member, IEEE) received the master's degree in 1986 and the Ph.D. degree in applied mathematics with a specialty in queuing theory from the University of Twente, The Netherlands, in 1990. He was a Researcher and a Program Manager with TNO from 1992 to 2009 with a focus on intelligent transport systems, where he was involved in various national and international projects. Since 2009, he has been a Full Professor with the Department of Transport and Planning, Delft University of Technology, with a focus on the impact of intelligent transport systems on mobility. His research interest includes advanced driver assistance systems.



Riender Happee received the M.Sc. degree in mechanical engineering and the Ph.D. degree from the Delft University of Technology (TU Delft), The Netherlands, in 1986 and 1992, respectively. He investigated road safety and introduced biomechanical human models for impact and comfort at TNO Automotive from 1992 to 2007. He currently investigates the human interaction with automated vehicles focussing on safety, comfort, and acceptance at the Delft University of Technology, where he is also an Associate Professor with the Faculties of Mechanical, Maritime and Materials Engineering, and Civil Engineering and Geosciences.